DOI: 10.21062/mft.2025.074 http://www.journalmt.com

Effect of Laser Shock Peening and Hot Isostatic Pressing on the Microstructure of MoNiCr Nickel Based Alloy

David Bricín (0000-0002-9354-2751)[1], Zbyněk Špirit (0000-0002-5676-1840)[1], Josef Strejciu[1], Antonín Kříž (0000-0001-8188-6621)[2]
[1]Centrum výzkumu Rez s.r.o., Morseova 1245/6, Pilsen, 30100, Czech Republic E-mail: david.bricin@cvrez.cz; zbynek.spirit@cvrez.cz; josef.strejcius@cvret.czujep.cz martin.novak1@ujep.cz
[2]Faculty of Mechanical Engineering, J. E. Purkyne University in Usti nad Labem. Pasteurova 3334/7, 400 01 Usti nad Labem. Czech Republic. E-mail: antonin.kriz@ujep.cz

This study aimed to evaluate the change in the microstructure of MoNiCr nickel-based alloy because of specimen surface modification by laser shock peening (LSP) followed by heat treatment using the hot isostatic pressing technology (HIP). Specimens which were cut from casted ingot had 7 mm in thickness and 117 mm in diameter. LSP surface modification was performed in a 60x60 mm square grid on the central part of each of them. Different values of laser power density in combination with or without tape or underwater condition were used for that operation. Specimens were then cut in half. One part each of them was left in LSP surface treatment conditions, and the other was heat-treated using HIP. Heat treatment was done in an argon atmosphere using 1050 °C temperature and 120 MPa pressure. Several microscopy techniques were used to evaluate changes in specimen's microstructure caused by LSP and HIP. Optical profilometer was used to evaluate change in surface roughness. Optical and scanning electron microscopes were used to evaluate surface microstructural changes caused by LSP and HIP. Metallography analysis was supplemented by HV0.01 microhardness measurement. The results of the experiment showed that LSP caused plastic deformation of the surface, which increased with the applied laser energy density and the number of passes. Microhardness increased due to LSP to a depth of 0.7 mm from the specimen's surface. The HIP process caused decrease in surface hardness and recrystallization of the grains structure in some cases.

Keywords: LSP, HIP, MoNiCr, Laser Shock Peening, Hot Isostatic Pressing

1 Introduction

Nickel alloys such as the MoNiCr alloy developed by Comtes FHT are among the candidates to produce components of molten-salt-cooled reactors, where, due to high operating temperatures and corrosively aggressive environments of fluoride or chloride salts, it is necessary to ensure sufficient corrosion resistance, creep resistance and sufficient strength [1, 2]. These components, which include the reactor vessel, piping systems, pumps, or valves, are often produced by casting, which is one of the cheap variants of their production. Casting can also produce relatively complicated shapes that would be difficult to produce using conventional forming techniques. The disadvantage of the components created in this way is that their structure is less resistant to corrosion damage or fatigue than the formed one due to many structural defects. The experiment aimed to verify the possibility of using laser shock peening technology in combination with hot isostatic pressing to create a recrystallized surface structure in the cast MoNiCr alloy, which could positively affect corrosion resistance and fatigue life of the casted component.

2 Material and Methods

Chemical composition of main alloying elements it is possible to find in table 1. Four samples were cut from them in dimension of 7 mm in thickness and 117 mm in diameter, see fig. 1.

Tab. 1 *Chemical composition of sample extracted from ingot measured by Energy Dispersive Spectroscopy*

Wt. %	Al	Mn	Si	Fe	Cr	Mo	Ni
Specimens	0.2±0.01	0.5±0.02	0.7±0.02	2.5±0.04	7.3±0.1	17.1±0.2	Rest

Specimens surface was polished to get similar initial roughness before application of surface treatment by LSP. LSP was done by Bivoj Laser in Hilase centre *(FZU, Dolní Břežany, CZE).* Parameters which were used are summarised in fig. 1. Specimens were then divided in half. One part each of them was kept with

surface modified by LSP the other was heat treated by HIP. HIP was done in argon atmosphere using 1050 °C temperature, holding time 1 hour, 120 MPa pressure and cooled by argon overpressure to room temperature. Surface topography and roughness were both analysed by Keyence VKX-100 profilometer *(Keyence, Mechelen, BE)*. Measurement was done using 20x objective with a pitch of 0.75 μm in the Z direction. Area of measurement was about 4.36x4.36 mm.

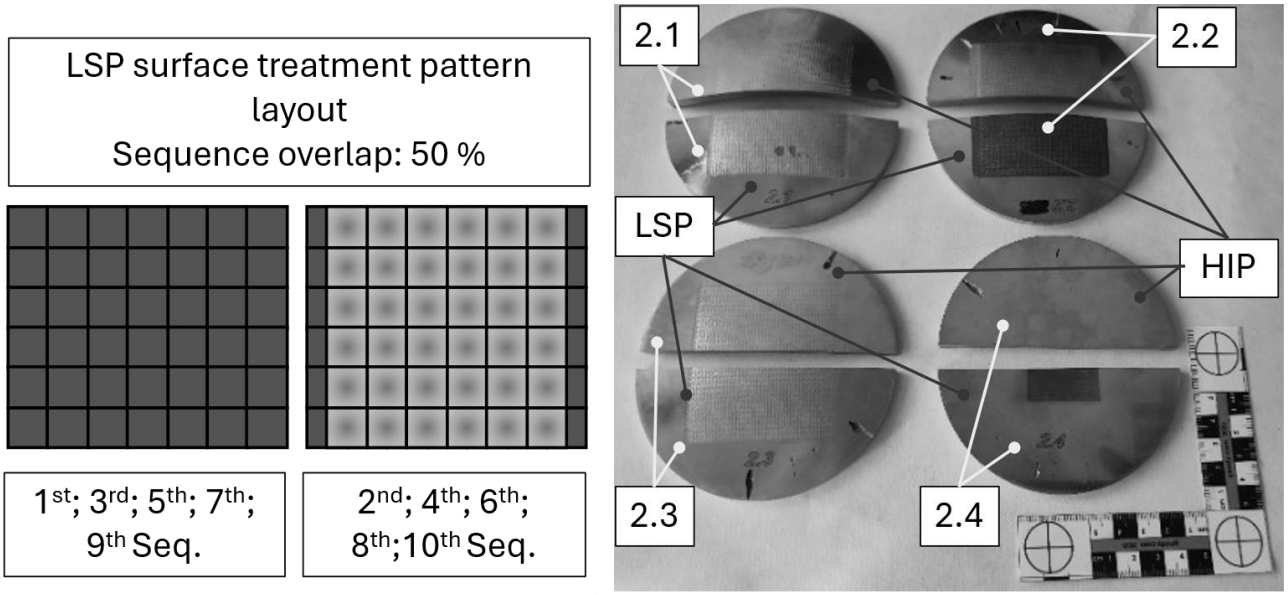

Sample	Pulse length [ns]	Power density [GW/cm²]	Number of sequences	Absorbing layer	Confining layer
2.1	10	8	10	Black tape	Flowing water
2.2	10	8	10	-	Flowing water
2.3	10	10	3	Black Tape	Flowing water
2.4	10	-	3	-	Under-water

Fig. 1 *LSP surface treatment specification and specimens' distribution*

Hardness profile measurement up to 1.5 mm bellow the specimens' surface with step of 0.05 mm between indentations was done by HV0.01 method using semiautomatic hardness tester Struers DuraScan (*Struers GmbH, Roztoky u Prahy, CZE)*. First indentation was done at 0.05 mm distance from edge of specimens' surface. The hardness profile curve for each specimen was created by averaging values from six profile measurements, three taken from each metallography cut. Metallography cuts were made in two perpendicular directions in the central part of each specimen. An etchant containing acetic acid, HNO_3, and HCL in a 1:1:1.5 ratio revealed the specimens' microstructure. Etching was done at room temperature and duration of 1 min. Tescan Mira 3 *(TESCAN ORSAY HOLDING, a.s., Brno, CZE)* scanning electron microscope (SEM) and light optical microscope CarlZeiss Observer Z1m *(Carl Zeiss s.r.o., Prague, CZE)* were used to analyse the microstructure changes caused by LSP and HIP in the areas close to the specimen's surface. SEM analysis was done using secondary electron (SE), backscattered electrons (BSE), and electron backscatter diffraction (EBSD) modes in combination with local analysis of chemical composition carried out by using Energy Dispersive Spectroscopy (EDS).

3 Results and discussion

As a result of the surface treatment of the LSP, samples 2.1, 2.2, and 2.3 underwent significant plastic deformation of their surfaces. This change is shown in Figure 2, The modified surface consisted of protrusions and grooves repeated at regular intervals. The distance between the highest and lowest point then varied according to the number of laser beam passes. In the case of the methods where the LSP process was repeated 10 times, the difference between the highest and lowest points was around 50 μm (2.1 and 2.2 samples). When repeating the process 3 times (2.3 Samples), the difference in heights was around 20 μm.

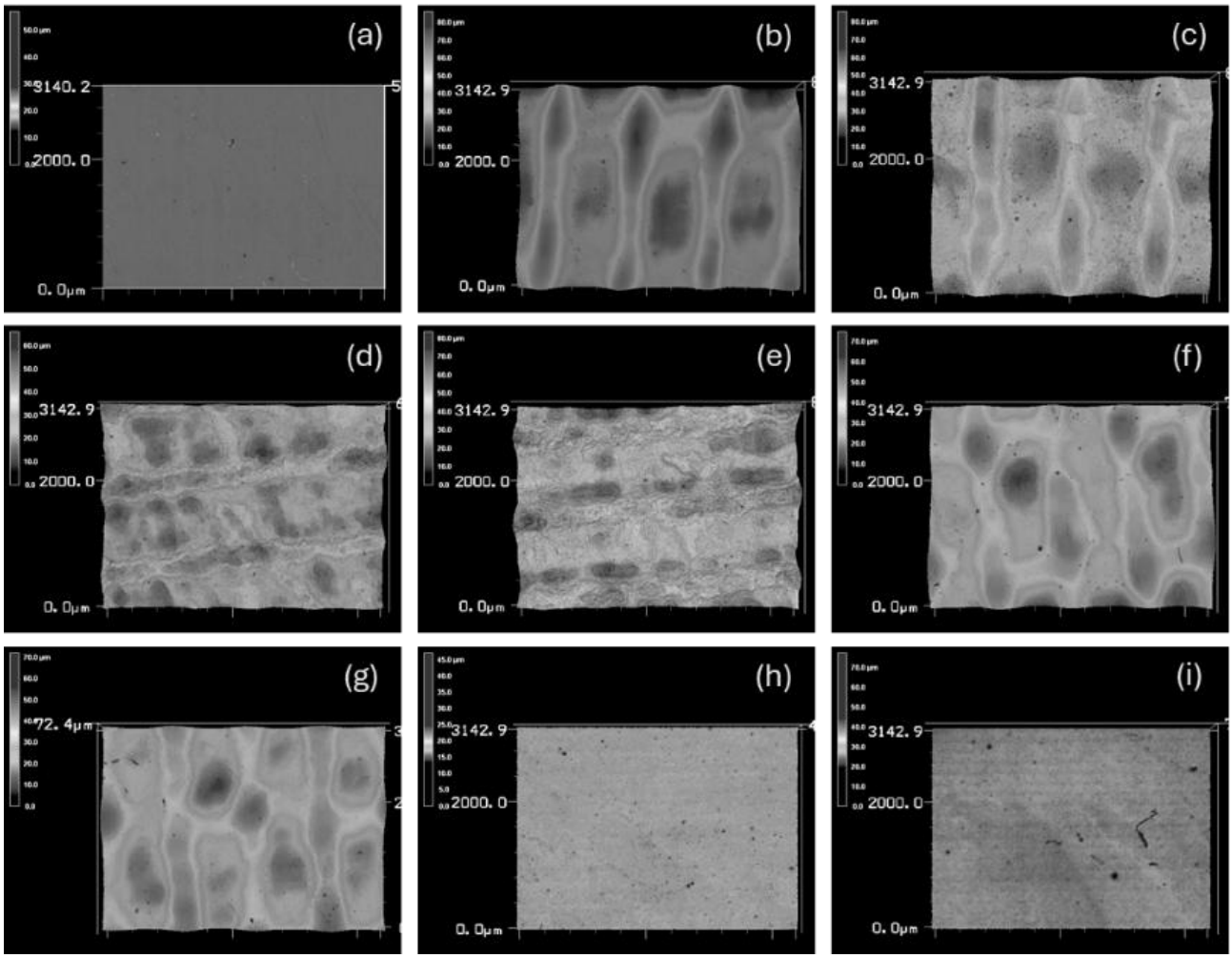

Fig. 2 *Surface topography height maps. (a) Initial surface; (b) 2.1_LSP; (c) 2.1_HIP; (d) 2.2_LSP; (e) 2.2_HIP; (f) 2.3_LSP; (g) 2.3_HIP; (h) 2.4_LSP; (i) 2.4_HIP*

In the case of LSP performed underwater (2.4 samples), the difference in profile heights was significantly smaller and was in the same range as in the case of the initial profile. The difference in their height was around 2 µm. Another observable change was an increase in the value of the roughness parameters for all LSP surface treatment variants, see table 2. The results also show that the HIP treatment did not cause a measurable change in the surface roughness parameters.

Tab. 2 *Roughness parameters value comparison*

	Ra [µm]	**Rp [µm]**	**Rv [µm]**	**Rz [µm]**
Initial values	0.3±0.1	2.1±1.7	1.4±0.2	3.5±1.6
21_LSP	7±2.6	18.3±6.5	13.6±5.3	31.9±11.8
21_HIP	4.8±1.8	14.6±6.1	11.9±3.2	26.5±9.3
22_LSP	5.9±1.4	17.7±5.3	13.8±1.6	31.5±6.6
22_HIP	6.8±3	19±7.8	17.5±4.7	36.5±12.5
23_LSP	5.3±1.4	14.7±3.5	10.6±2.6	25.3±5.9
23_HIP	5.2±1.7	14.1±3.5	11.7±2.2	25.7±5.7
24_LSP	0.9±0.03	4.3±0.5	4±0.5	8.3±0.7
24_HIP	0.9±0.1	3.7±0.2	3.9±0.3	7.6±0.3

The change in surface topography associated with increased surface roughness of the samples is a frequently described phenomenon related to the LSP process [3]. The effect of energy density is often mentioned, where higher values of energy density led to higher plastic reshaping of the surface and an increase in surface roughness [4]. Similarly, multiple sequences of pulse laser passes, as in the case of this and other studies [5, 6], have a similar effect. HIP processing did not affect the achieved roughness, similarly as in

study [7]. The processing takes place under a protective atmosphere, thus limiting the formation of oxide layers that could affect the surface roughness. The roughness evaluation was performed outside the region of casting defects, where the surface may be reshaped as in the case of printed parts, and this may be reflected in a change in surface roughness, as mentioned in ref [8]. Results of microhardness analysis are summarised in Fig. 3.

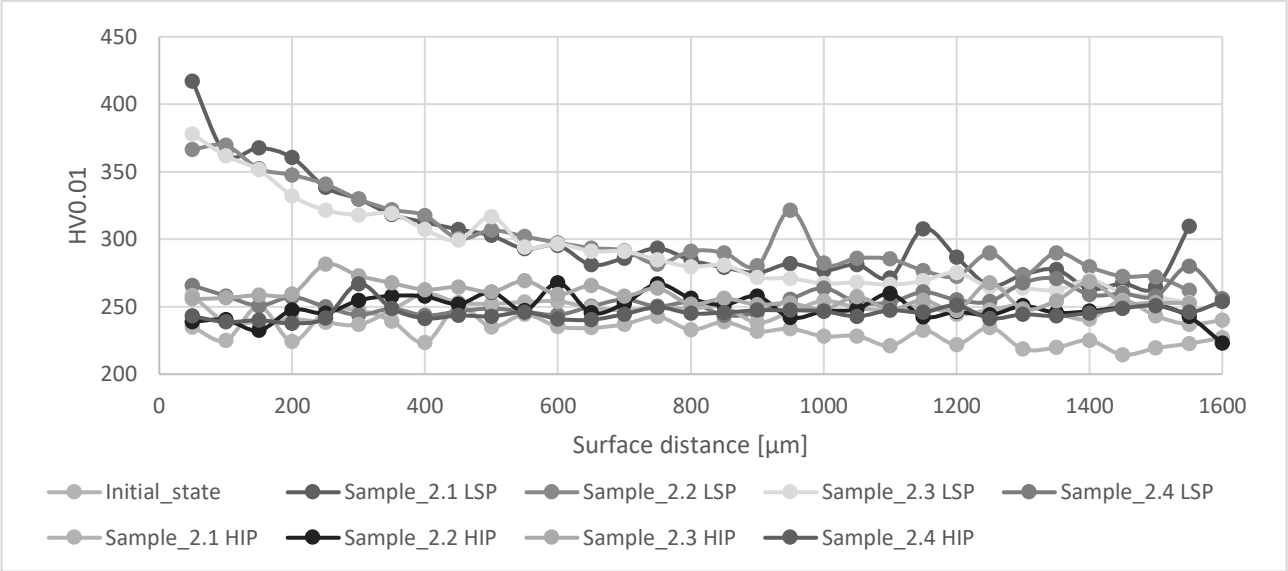

Fig. 3 *HV0.01 microhardness profiles*

LSP caused an increase in hardness up to 417±35HV0.01, 367±20HV0.01 and 378±19HV0.01 in 0.05 mm distance from the surface in the case of the 2.1, 2.2 and 2.3 Specimens. Microhardness then gradually decreased up to 279±10HV0.01 in distance approximately 0.5 mm from the specimen's surface. Profile of microhardness had then almost linear trend in all measurement points. Same linear trend in microhardness was possible to observe in case of initial state specimens, HIP treated specimens and 2.4 specimens after LSP. Average value of microhardness for those specimens was about 251±7HV0.01.The Microhardness increase in the surface layer after LSP surface treatment is associated with an increase in the residual compressive stresses acting in this area [9, 10]. Residual compressive stresses then acting in surface layer have a positive effect on the fatigue life because they limit the development of fatigue damage, which mainly arises from surface notches or structural defects near the surface. The decrease in the microhardness after HIP processing is then related to the microstructural rearrangement associated with annihilation by dislocation [11].

Figure 4 shows a comparison of the structure at the surface of the samples. From the images, it can be seen that the grains have a dendritic structure, which is evident both in the samples after LSP and in the samples that were further processed by HIP technology.

In the samples after HIP treatment, areas of polygonal grains were observed near their surface. These areas were compact in the case of sample groups 2.1 and 2.2. In the case of sample group 2.1, the average depth to which this area extended was around 458±51 um, while in the case of sample group 2.2, it was around 290±71 um. In the case of sample group 2.3, the layer formed was not compact. Its depth was around 208+-92 um. In the case of the samples of group 2.4, this area was not observed as in the case of the samples after LSP and the samples without surface treatment. Figures 5 and 6 show a comparison of the grain structure orientation in specimen regions close to the surface using IPF and GOS maps.

The GOS maps show an increase in the average value of grain orientation spread after LSP surface treatment, with this value being around 1.3°-1.9° see Table X. As a result of HIP, this value then decreases and reaches a value of around 0.4°-0.5° at most measured points in the region of new grain formation, which is closed to 0.6° the value obtained for the untreated samples. The IPF maps show the scatter in the orientation of the individual grains in this region. The formation of the new sample structure caused by HIP treatment was accompanied by an increase in the proportion of high-angle grain boundaries (HAGB) and a decrease in the proportion of low-angle and ultra-low angle grain boundaries (LAGB and ULAGB), see Table 3. The data in the table also show that the grain size decreased due to the formation of new recrystallized grains near the surface of the samples. It is also evident from the data that the recrystallization of the structure in the surface layer led to a decrease in the density of dislocations in this region, which increased during the LSP processing of the sample surface.

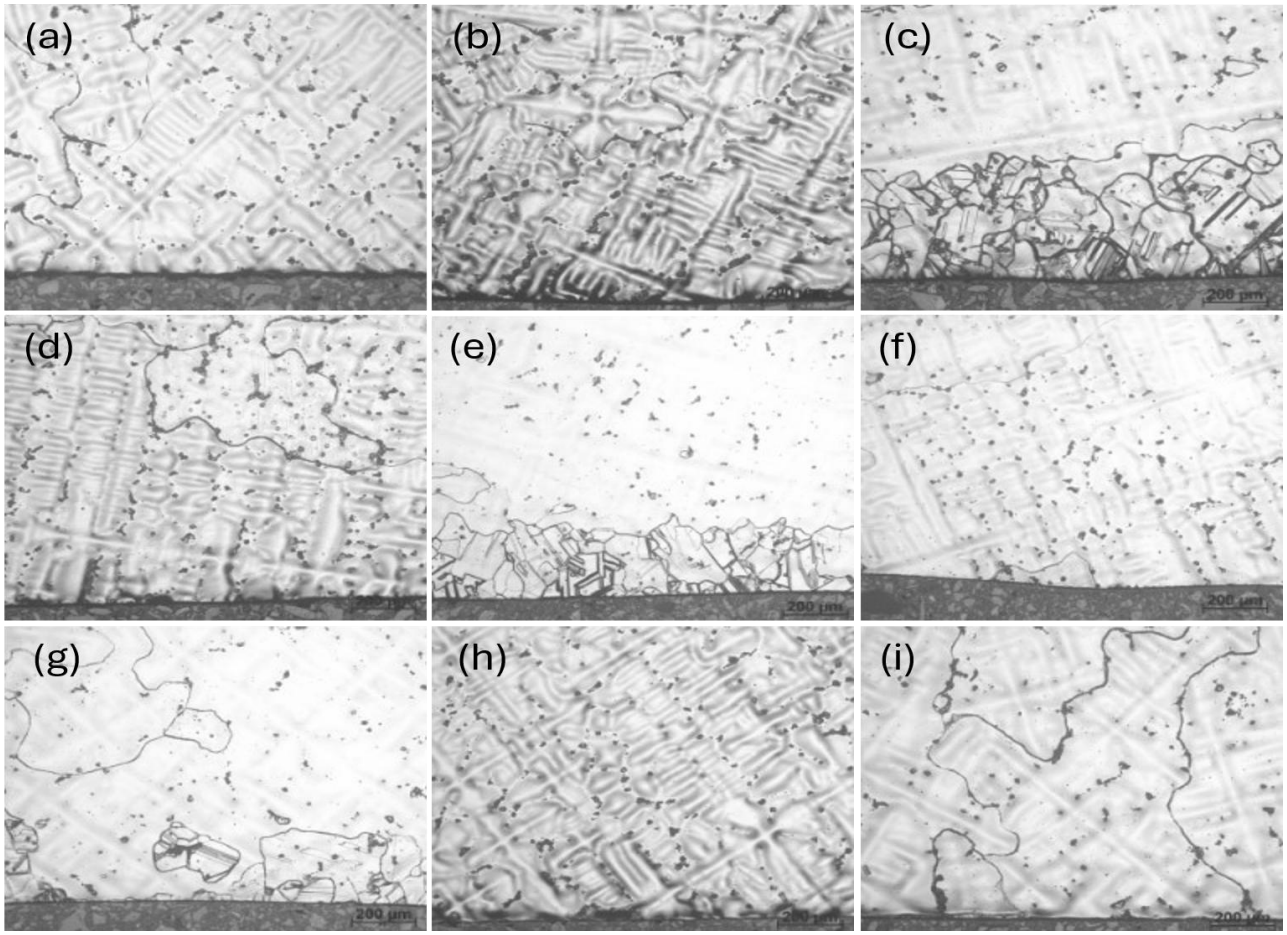

Fig. 4 *LOM samples microstructure comparison; (a) Initial state; (b) 2.1_LSP; (c) 2.1_HIP; (d) 2.2_LSP; (e) 2.2_HIP; (f) 2.3_LSP; (g) 2.3_HIP; (h) 2.4_LSP; (i) 2.4_HIP*

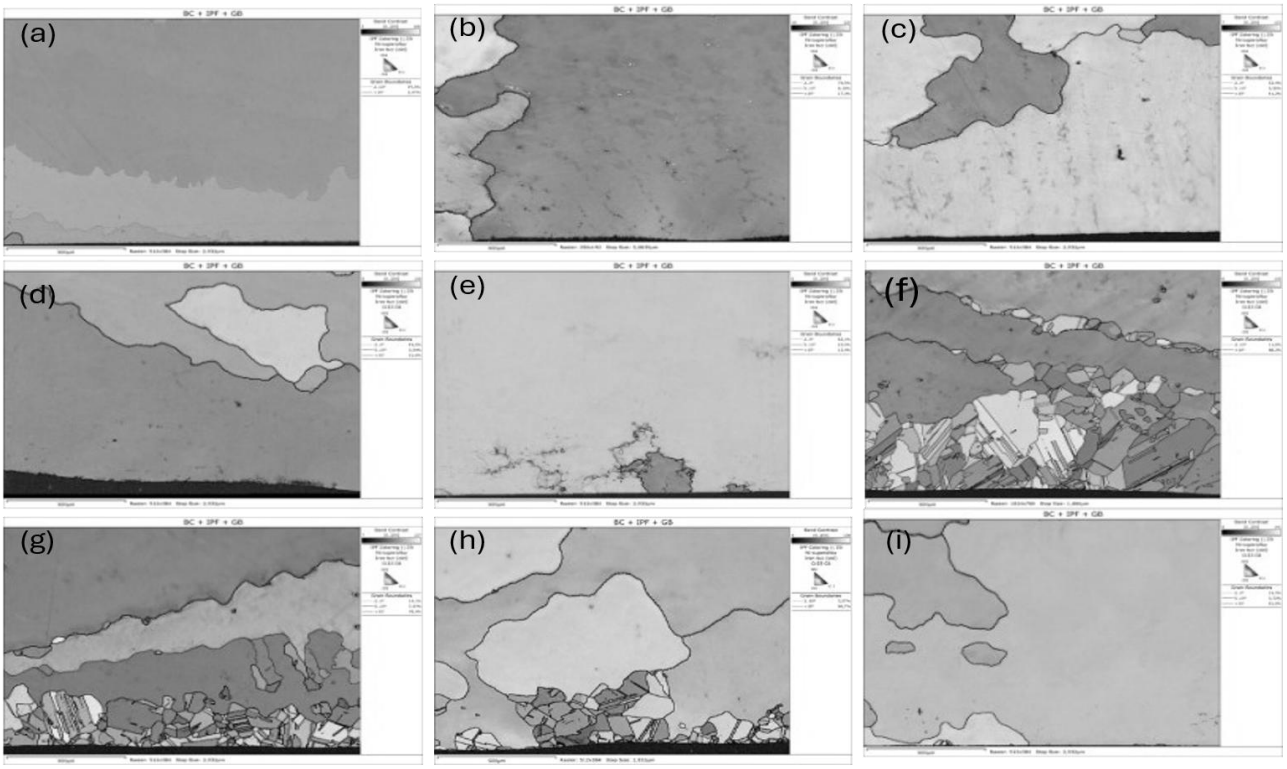

Fig. 5 *IPF+GB maps comparison; (a) Initial state; (b) 2.1_LSP; (c) 2.1_HIP; (d) 2.2_LSP; (e) 2.2_HIP; (f) 2.3_LSP; (g) 2.3_HIP; (h) 2.4_LSP; (i) 2.4_HIP*

In the dendritic structure of the analysed nickel alloy, there is an increase in the density of dislocations in the regions between the grain boundaries and in the areas between the dendrite branches [12]. This is related to the tendency for crystallographic defects to accumulate in these regions. Because of LSP processing, the movement of dislocations occurs with the increase in strain and strain rate, forming a dislocation network and dislocation walls in these regions. If the strain is large enough, sub-grain boundaries or grain boundaries with high misorientation are formed in the dislocation wall locations. In this case, the nucleation of new grain boundaries occurred because of subsequent processing of the samples using HIP technology, where recrystallization was promoted by the high temperature and pressure of the process used. The areas of new grain formation are then clearly visible in the above images, see Figures 5-6.

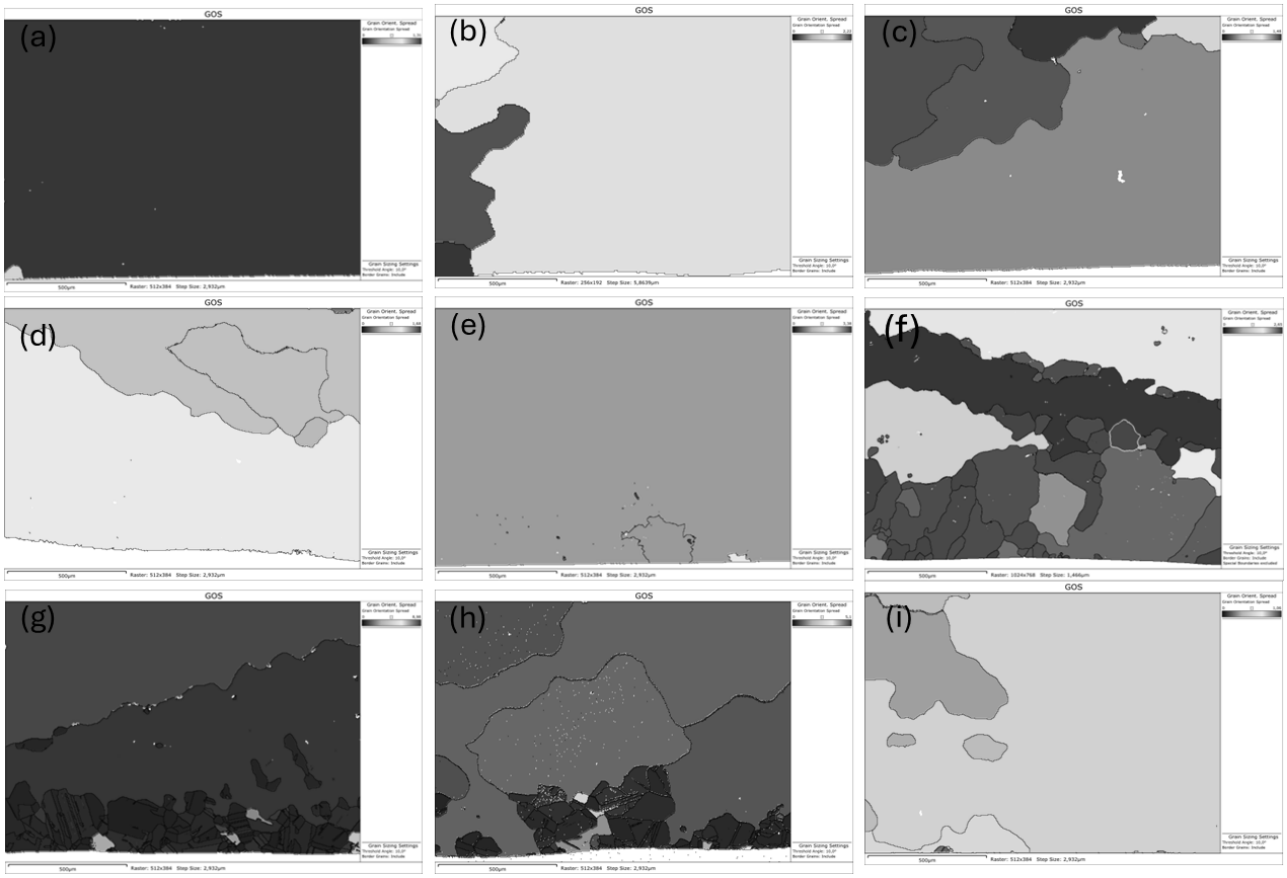

Fig. 6 *GOS maps comparison; (a) Initial state; (b) 2.1_LSP; (c) 2.1_HIP; (d) 2.2_LSP; I 2.2_HIP; (f) 2.3_LSP; (g) 2.3_HIP; (h) 2.4_LSP; (i) 2.4_HIP*

Tab. 3 *EBSD results (ULAGB means Ultra-Low Angle Grain Boundaries; LAGB means Low Angle Grain Boundaries; HAGB means High Angle Grain Boundaries)*

Sample	ULAGB	LABG	HAGB	Grain size [μm]	GND [x10^{14}/m^2]	GOS [°]
	2°-5°	5°-15°	15°<			
I_S	54.8±26.4	9.9±2.9	34.3±22.9	409±361	1.9±0.7	0.6±0.4
21_LSP	73.8	8.6	17.6	457±356	4.2±1.3	1.7±0.3
21_HIP	7.2±3.6	2±0.8	90.8±4.4	92±83	2.6±0.7	0.5±0.3
22_LSP	56.3±2.9	4.8±0.5	38.7±2.5	324±292	3.9±1.1	1.9±0.5
22_HIP	12.4±1.8	5±2.4	82.6±4.2	98±82	2.7±0.8	0.4±0.0
23_LSP	54.7±9.7	5.1±1.7	40.2±11.4	436±388	4.3±1.1	1.4±0.5
23_HIP	1.8±0.3	6.5±1.4	91.8±1.1	59±51	2.3±0.7	0.3±0.1
24_LSP	75.7±13.1	13±7.2	11.3±5.9	404±521	2.2±0.7	1.3±0.6
24_HIP	18.1±2.8	4.4±0.7	77.6±3.4	173±212	2.2±0.7	0.4±0.1

4 Conclusion

The experimental results show that using LSP it is possible to increase the dislocation density and acting residual stresses in the surface of the samples in such a way that during subsequent HIP processing, the grain structure in the surface layer of the cast MoNiCr alloy will recrystallize. According to the presented results, the degree of this recrystallization depends on the number of repetitions of laser pulse passes, their energy density, and the used confining layer. For the needs of development in the areas of MSR, it will be necessary to carry out experiments where, for example, the corrosion stability of the recrystallized layer or fatigue life will be evaluated.

Acknowledgement

The presented work has been realized within Institutional Support by Ministry of Industry and Trade of the Czech Republic with the usage of CICRR infrastructure.

References

[1] FULÍN, Z., STREJCIUS, J. & ŠPIRIT, Z. Corrosion of Inconel 800HT Alloy in Molten Fluoride Salts. *Manufacturing Technology*, 2024, 24, 755-64. doi: 10.21062/mft.2024.087

[2] MURÁNSKY, O. ET AL. Molten salt corrosion of Ni-Mo-CR candidate structural materials for Molten Salt Reactor (MSR) systems, *Corrosion Science*, 2019, 159, p. 108087. doi:10.1016/j.corsci.2019.07.011.

[3] DENG, W. ET AL. Progressive Developments, challenges and future trends in laser shock peening of metallic materials and alloys: A comprehensive review, *International Journal of Machine Tools and Manufacture*, 2023, 191, p. 104061. doi:10.1016/j.ijmachtools.2023.104061.

[4] MALEKI, E. ET AL. The effects of shot peening, laser shock peening and ultrasonic nanocrystal surface modification on the fatigue strength of Inconel 718, *Materials Science and Engineering: A*, 2021, 810, p. 141029. doi:10.1016/j.msea.2021.141029.

[5] LU, J.Z. ET AL. Effects of multiple Laser Shock Processing (LSP) impacts on mechanical properties and wear behaviors of AISI 8620 Steel, *Materials Science and Engineering: A*, 2012, 536, pp. 57–63. doi:10.1016/j.msea.2011.12.053.

[6] LARSON, E.A. ET AL. Optimize multiple peening effects on surface integrity and microhardness of aluminum alloy induced by LSP', *Materials Sciences and Applications*, 2023, 14(03), pp. 208–221. doi:10.4236/msa.2023.143012.

[7] MASUO, H. *ET AL.* Effects of defects, surface roughness and hip on fatigue strength of ti-6al-4v manufactured by additive manufacturing', *Procedia Structural Integrity*, 2017, 7, pp. 19–26. doi:10.1016/j.prostr.2017.11.055.

[8] SUN, L. ET AL. Influencing mechanisms of hot isostatic pressing on surface properties of additively manufactured alsi10mg alloy, *Journal of Materials Processing Technology*, 2024, 329, p. 118426. doi:10.1016/j.jmatprotec.2024.118426.

[9] KAUFMAN, J. *ET AL.* Mitigating environmental assisted cracking in heterogeneous welds by laser peening without coating, *Engineering Failure Analysis*, 2025, 167, p. 108982. doi:10.1016/j.engfailanal.2024.108982.

[10] [ZHANG, H. *ET AL.* The effect of laser shock peening with different power density on the microstructure evolution and mechanical properties of Mar-M247 nickel-base alloy, *Journal of Materials Research and Technology*, 2024, 30, pp. 3340–3354. doi:10.1016/j.jmrt.2024.04.107.

[11] REN, D. *ET AL.* Effect of hot isostatic pressing on the mechanical and corrosive properties of ti–ni alloy fabricated by selective laser melting', *Journal of Materials Research and Technology*, 2023, 26, pp. 4595–4605. doi:10.1016/j.jmrt.2023.08.197.

[12] LIU, G. *ET AL.* The effects of grain size, dendritic structure and crystallographic orientation on fatigue crack propagation in IN713C nickel-based superalloy, *International Journal of Plasticity*, 2020, 125, pp. 150–168. doi:10.1016/j.ijplas.2019.09.010.